Acta Cryst. (1995). D**51**, 842–844

Preliminary crystallographic analysis of chloroperoxidase from *Caldariomyces fumago*.

By MUNIRATHINAM SUNDARAMOORTHY, *Departments of Molecular Biology and Biochemistry, and Physiology and Biophysics, University of California at Irvine, Irvine, CA* 92717-3900, *USA*, J. MATTHEW MAURO,* *Center for Advanced Research in Biotechnology of the Maryland Biotechnology Institute*, 9600 *Gudelsky Drive, Rockville, MD* 20850, *USA*, ANN M. SULLIVAN and JAMES TERNER, *Department of Chemistry, College of Humanities and Sciences, Virginia Commonwealth University, Box* 2006, 1001 *West Main Street, Richmond, VA* 23284, *USA*, and THOMAS L. POULOS,† *Departments of Molecular Biology and Biochemistry, and Physiology and Biophysics, University of California at Irvine, Irvine, CA* 92717-3900, *USA*

(*Received* 28 *June* 1994; *accepted* 24 *January* 1995)

Abstract

Chloroperoxidase from the fungus *Caldariomyces fumago* has been crystallized in two space groups, $C222_1$ and $P2_12_12_1$ both of which are suitable for high-resolution X-ray studies. Parent data sets have been obtained to 2.16 Å in space group $C222_1$ and 2.00 Å in space group $P2_12_12_1$. Heavy-atom derivatives have been obtained with both forms and electron-density maps calculated. The heme has been located and continuous electron density between the heme and protein clearly indicates the location of the proximal ligand.

Introduction

Chloroperoxidase (CPO) from the fungus *Caldariomyces fumago* is one of the most diverse of the known heme enzyme catalysts (Griffin, 1991) and exhibits peroxidase, catalase and cytochrome *P*450-like activities. CPO consists of a single glycosylated 300-residue polypeptide chain (Fang, Kenigsberg & Hager, 1986) with a single iron protoporphyrin IX as the prosthetic group (Morris & Hager, 1966). CPO appears to be a hybrid of cytochromes *P*450 and peroxidases. Like *P*450, CPO is thought to have a cysteine residue as the proximal heme ligand (Hollenberg & Hager, 1973; Bagcharoenpaurpong, Champion, Hall & Hager, 1986; Blanke & Hager, 1988); rather than histidine, as is the case with most heme peroxidases. However, like peroxidases, CPO is thought to have a distal pocket containing acid–base catalytic groups, possibly histidine, (Sono, Dawson, Hall & Hager, 1986) while *P*450 has a hydrophobic pocket without a catalytic histidine (Poulos, Finzel & Howard, 1987). Thus, CPO occupies a unique niche amongst heme enzymes and one would expect that the breadth of activities exhibited by CPO will be reflected by some interesting and novel structural features.

CPO was first crystallized in 1966 (Morris & Hager, 1966) but these crystals proved unsuitable for diffraction studies. Rubin, Van Midelworth, Thomas & Hager (1982) reported a new crystal form that appeared to be suitable for structure determination. However, no further work with these crystals has been reported. Using various CPO preparations, we have not been able to obtain the crystals described by Rubin *et al.* (1982). The reasons remain unknown but we suspect that the nature of the growth conditions used for cultivating the organism and the extent and type of glycosylation may be a factor. We now find that CPO prepared in large quantities for resonance Raman studies crystallizes in two forms, one of which is isomorphous with those reported by Rubin *et al.* (1982) and both of which are suitable for crystallographic studies.

Results and discussion

Protein purification

C. fumago, strain ATCC 16373 (American Type Culture Collection, Rockville, MD), was immobilized and grown in a high-fructose growth medium (Pickard, 1981) within aerated and rotating carboys following the procedure of Blanke, Yi & Hager (1989). After 8 d the growth medium containing the chloroperoxidase or CPO was collected, concentrated and subjected to ethanol fractionation to remove the gelatinous black pigment. The CPO fraction was chromatographed over a DEAE–Sepharose Fast Flow (Pharmacia) ion-exchange column using linear gradients of 5 to 500 m*M* sodium acetate, pH = 3.8. The CPO eluted at approximately 50 m*M* buffer and was next absorbed to a CM–Sepharose column and chromatographed using a 5 to 500 m*M* gradient in the same acetate buffer. The CPO eluted at approximately 15 m*M*. Other CPO isozymes either did not absorb to either the DEAE or CM columns, or eluted only at high ionic strength.

Crystallization

Diffraction-quality crystals were obtained using seeding techniques (Stura & Wilson, 1991) in three separate steps.

Step 1. *Spontaneous crystallization.* The hanging-drop method using Linbro plates was used for all crystallizations at room temperature. The well solution consisted of 20% PEG 6000, 0.31 *M* NaCl (LiCl or KCl also worked), and 0.01 *M* potassium phosphate, pH 6.0. The protein drop consisted of an equal volume of well solution and 10 mg ml^{-1} protein in 0.01 *M* phosphate, pH 3.7. Crystals grew as long, thin needles within 3–5 d.

Step 2. *Microseeding.* The same experiment as in step 1 was repeated except the final CPO concentration was lowered to 2–3 mg ml^{-1}. After equilibrating for 3–4 d as a hanging drop, the protein drop was touch seeded as follows. A thin metal wire was used to touch the surface of a drop containing the needle crystals prepared in step 1 and then to a fresh protein drop. Crystals about 0.15 mm in the longest dimension grew in about one week.

Step 3. *Macroseeding.* Small crystals obtained in step 2 were successively washed with 26, 24 and then 22% PEG 6000 containing 0.31 *M* NaCl and 0.01 *M* potassium phosphate, pH 6.0. A washed crystal was transferred to a protein drop prepared

* Present address: Center for Biomolecular Science and Engineering, 10903 Indian Head Highway, Fort Washington, MD 20744, USA.

† To whom correspondence should be addressed.

Table 1. *Summary of data collection for parent crystals*

Space group	Resolution (Å)	$I/\sigma(I)$*	Total obs.	Unique data	% Complete	R_{symm}†
$C222_1$	2.16	1.13	195731	26846	98	0.105
$P2_12_12_1$	2.00	1.63	171375	26188	98	0.079

* I/σ = ratio of intensity (I) to background at highest resolution.
† $R_{symm} = \sum_h \sum_i |\langle I(h)\rangle - I(h)_i| / \sum_h \sum_i I(h)_i$ for symmetry-related reflections.

Table 2. *Summary of data collection for heavy-atom derivative crystals*

Derivative	Resolution (Å)	$I/\sigma(I)$	Total obs.	Unique data	% Complete	R_{symm}	R_{merge}*
$GdCl_3$	2.70	1.9	134468	12568	100	0.071	0.156
$Sm(NO)_3$	2.77	1.5	144554	11323	76	0.071	0.107
K_2PtCl_4	2.70	1.0	174248	12940	100	0.080	0.111
K_2PtCl_6	2.80	1.0	101812	11642	100	0.077	0.103
$K_2Pt(NH_2)_2Cl_2$	2.60	1.8	88307	13344	61	0.064	0.098
KI_3	2.95	1.3	88281	9753	100	0.064	0.153
HMPS	2.75	1.1	102605	12348	100	0.073	0.170

* $R_{merge} = \sum_h |F_{PH} - F_P| / \sum_h F_P$, where F_P and F_{PH} are the native and derivative structure-factor amplitudes, respectively.

Table 3. *Summary of phase calculations*

Derivative	No. of sites	R_{Cullis}*	Phasing power† Overall	At 3.0 Å
$GdCl_3$	1	0.688	1.54	1.36
$Sm(NO)_3$	1	0.659	1.65	1.39
K_2PtCl_4	3	0.586	1.64	1.20
K_2PtCl_6	1	0.656	0.94	0.70
$K_2Pt(NH_2)_2Cl_2$	1	0.721	0.73	0.53
KI_3	2	0.669	0.67	0.58
HMPS	2	0.764	0.44	0.37
$GdCl_3$ anomolous	1		1.34	1.05
Native anomolous	1		0.99	0.86

* $R_{cullis} = \sum ||F_{PH} \pm F_H| - F_H| / \sum |F_{PH} \pm F_P|$.
† Phasing power $= F_H(\text{calc})/E$, where $F_H(\text{calc})$ is the calculated scattering amplitude for the heavy-atom structure, and E is the estimated lack-of-closure error.

and equilibrated as in step 2. Crystals measuring 0.7 × 0.3 × 0.2 mm grew in about two weeks. This procedure is very reproducible and routinely gives high-quality crystals that are stable for several days in the X-ray beam.

Data collection

Crystals were characterized using a Siemens area-detector system and a rotating-anode X-ray source equipped with focusing optics. Initially these crystals were indexed in space group $P2_1$ with two CPO molecules per asymmetric unit. Subsequent analysis, however, showed that the data also could be indexed in the higher symmetry space group, $C222_1$, with unit-cell dimensions $a = 58.43$, $b = 152.76$ and $c = 102.29$ Å and one CPO molecule per asymmetric unit. This is the same space group and cell dimensions reported by Rubin *et al.* (1982). In the course of searching for heavy-atom derivatives, we were concerned that the high concentration of NaCl might interfere with heavy-atom binding. Crystallization trials were carried out as described above except NaCl was excluded. By excluding NaCl and by increasing the PEG 6000 concentration to 30%, a new crystal form was obtained. These crystals belong to space group $P2_12_12_1$ with unit-cell dimensions $a = 58.77$, $b = 71.36$ and $c = 91.73$ Å with one molecule per asymmetric unit. Micro- and/or macroseeding were not required to obtain high-quality crystals.

Parent data sets have been obtained for both forms (Table 1). The $P2_12_12_1$ form diffracts to higher resolution and will be used for the high-resolution refinement. Since it should be possible to average electron-density maps in the two space groups and hence, improve map quality (Bricogne, 1976), heavy-atom searches are being pursued in both crystal forms. Thus far, interpretable difference Patterson maps have been obtained in both crystal forms with $GdCl_3$, K_2PtCl_4 and *p*-hydroxymercuricphenylsulfonic acid (HMPS). In addition,

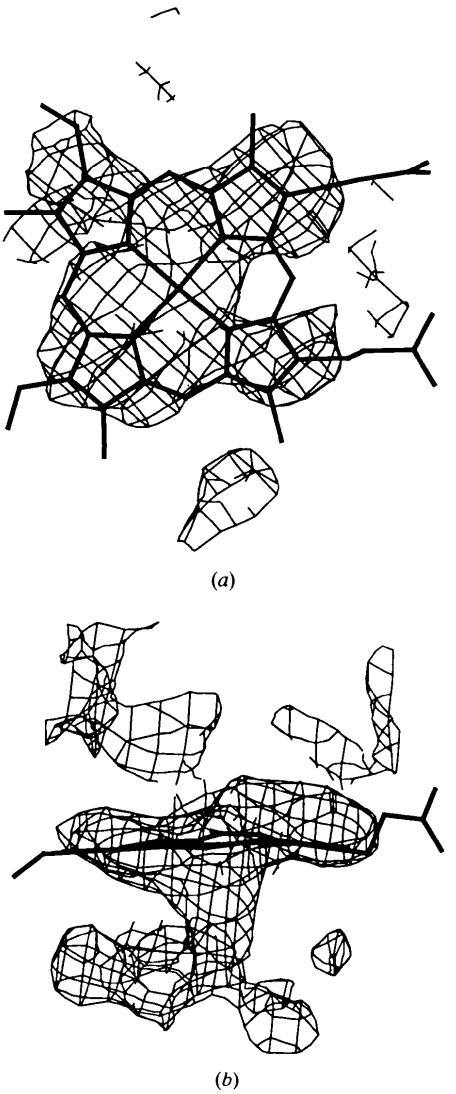

Fig. 1. The solvent-leveled MIR map contoured at 1σ (σ = root-mean-square electron density over an asymmetric unit) in the vicinity of the heme. The top (*a*) and side (*b*) views are shown. Note that in the side view, the continuous electron density between the protein and heme clearly indicates the location of the proximal heme ligand. Heavy-atom positional parameters and phases were calculated with the *PHASES* package of programs (Furrey & Swaminathan, 1990) and solvent leveling was carried out using a modified version of B. C. Wang's procedure (Wang, 1985) as implemented in the *PHASES* package.

derivatives have been obtained in the $C222_1$ form with K_2PtCl_6, $Pt(NH_4)_2Cl_2$, $Sm(NO_3)_3$ and KI_3. Also, the anomolous data from the native crystal, which has a heme iron, and the $GdCl_3$ derivative will be used for phasing. The gadolinium and samarium derivatives share the same site and hence are not independent derivatives. Similarly, the independent platinum sites in $Pt(NH_4)_2Cl_2$ and K_2PtCl_6 derivatives are shared by K_2PtCl_4 derivative. The data-collection and phasing statistics are given in Tables 2 and 3, respectively, for the derivatives in the $C222_1$ form. Though the phasing power is very poor for $Pt(NH_4)_2Cl_2$, KI_3 and HMPS derivatives, the map does show a big improvement when these derivatives are included in phasing. Further, the gadolinium and samarium derivatives, along with the gadolinium anomalous data, dominate phasing.

An MIR (multiple isomorphous replacement) map has been obtained in both crystal forms and both are of about equal quality. For the $C222_1$ form, the overall figure of merit for 9186 reflections to 3.0 Å is 0.737. The heme has been located and in Fig. 1 is shown the solvent-leveled MIR map in the vicinity of the heme group. It already is clear that the structure of the heme pocket is quite different to the known heme peroxidase structures of cytochrome *P*450. We anticipate that CPO will reveal some new and unique structural features related to its unusually broad range of activities.

This work was supported by National Science Foundation Grant MCB 9296126 (TLP) and National Institutes of Health Grant GM34443 (JT).

References

BAGCHAROENPAURPONG, O., CHAMPION, O. M., HALL, K. S. & HAGER, L. P. (1986). *Biochemistry*, **25**, 2374–2378.

BLANKE, S. R. & HAGER, L. P. (1988). *J. Biol. Chem.* **263**, 18739–18743.

BLANKE, S. R., YI, S. & HAGER, L. P. (1989). *Biochemistry Lett.* **11**, 769–774.

BRICOGNE, G. (1976). *Acta Cryst.* A**32**, 832–847.

DAWSON, J. H., KAU, L.-S., PENNER-HAHN, J. E., SONO, M., EBLE, K. S., BRUCE, G. S., HAGER, L. P. & HODGSON, K. O. (1986). *J. Am. Chem. Soc.* **108**, 8114–8116.

FANG, G.-H., KENIGSBERG, P. & HAGER, L. P. (1986). *Nucleic Acids Res.* **14**, 8061–8071.

FURREY, W. & SWAMINATHAN, S. (1990). 14th Am. Crystallogr. Assoc. Meet. New Orleans. Abstract PA33.

GRIFFIN, B. W. (1991). In *Peroxidases in Chemistry and Biology*, Vol. II, edited by J. EVERSE, K. E. EVERSE & M. B. GRIFFIN, pp. 85–137. CRC Press.

HOLLENBERG, P. F. & HAGER, L. P. (1973). *J. Biol. Chem.* **248**, 2630–2633.

MORRIS, D. R. & HAGER, L. P. (1966). *J. Biol. Chem.* **241**, 1763–1768.

PICKARD, M. A. (1981). *Can. J. Microbiol.* **27**, 1298–1305.

POULOS, T. L., FINZEL, B. C. & HOWARD, A. J. (1987). *J. Mol. Biol.* **195**, 687–700.

RUBIN, B., VAN MIDLEWORTH, J., THOMAS, K. & HAGER, L. (1982). J. Biol. Chem. **257**, 7768–7769.

SONO, M., DAWSON, J. H., HALL, K. & HAGER, L. P. (1986). *Biochemistry*, **25**, 347–356.

STURA, E. A. & WILSON, I. A. (1991). *J. Cryst. Growth*, **110**, 270–282.

WANG, B. C. (1985). *Methods Enzymol.* **115**, 90–112.